Cub domain containing protein 1 (CDCP1) negatively regulates TGFβ signaling and myofibroblast differentiation

Nina Noskovičová[1], Katharina Heinzelmann[1*], Gerald Burgstaller[1], Jürgen Behr[2,3], and Oliver Eickelberg[1,4*]

*Oliver Eickelberg and Katharina Heinzelmann contributed equally to this work

[1]Comprehensive Pneumology Center, University Hospital of the Ludwig-Maximilians-University (LMU) Munich and Helmholtz Zentrum München, Member of the CPC-M BioArchive, Member of the German Center for Lung Research (DZL), Munich, Germany

[2]Asklepios Fachkliniken München-Gauting, Munich, Germany

[3]Medizinische Klinik und Poliklinik V, Klinikum der Ludwig-Maximilians-Universität (LMU), Munich, Germany

[4]Division of Respiratory Sciences and Critical Care Medicine, University of Colorado, Denver, CO, USA

To whom correspondence and requests should be addressed:
Oliver Eickelberg, Division of Respiratory Sciences and Critical Care Medicine, University of Colorado, Denver, CO, USA, Anschutz Medical Campus, 12700 E. 19th Avenue, RC 2, Room 9C03, Box C272, Aurora, CO 80045, (303)724-4075 (Phone), (303)724-6042 (Fax); Email: oliver.eickelberg@ucdenver.edu

Running title: *CDCP1 in myofibroblast transdifferentiation*

Keywords: fibroblast, myofibroblast differentiation, cell surface, cell signaling, transforming growth factor beta

ABBREVIATIONS

CDCP1	cub domain containing protein 1
TGFβ1	transforming growth factor-beta 1
phLFs	primary human lung fibroblasts
ECM	extracellular matrix
αSMA	alpha-smooth muscle actin
pSmad3	phosphorylated Smad3
PAR1	protease-activated receptor-1
PAR2	protease-activated receptor-2
MMP	matrix metalloproteinase
Sis3	specific inhibitor of Smad3
HPRT	hypoxanthine-guanine phosphoribosyltransferase
BZ	bortezomib

ABSTRACT

Fibroblasts are thought to be the prime cell type for producing and secreting extracellular matrix (ECM) proteins in the connective tissue. The profibrotic cytokine, transforming growth factor-beta 1 (TGFβ1) activates and transdifferentiates fibroblasts into αSMA-expressing myofibroblasts, which exhibit increased ECM secretion, in particular collagens. Little information, however, exists about cell-surface molecules on fibroblasts that mediate this transdifferentiation process. We recently identified, using unbiased cell-surface proteome analysis, Cub domain containing protein 1 (CDCP1) to be strongly downregulated by TGFβ1. CDCP1 is a transmembrane glycoprotein, the expression and role of which has not been investigated in lung fibroblasts to date. Here, we characterized, in detail, the effect of TGFβ1 on CDCP1 expression and function, using immunofluorescence, FACS, immunoblotting, and siRNA-mediated knockdown of CDCP1. CDCP1 is present on interstitial fibroblasts, but not myofibroblasts, in the normal and IPF lung. *In vitro,* TGFβ1 decreased CDCP1 expression in a time-dependent manner by impacting mRNA and protein levels. Knockdown of CDCP1 enhanced a TGFβ1-mediated cell adhesion of fibroblasts. Importantly, CDCP1-depleted cells displayed an enhanced expression of profibrotic markers, such as collagen V or αSMA, which was found to be independent of TGFβ1. Our data show, for the very first time, that loss of CDCP1 contributes to fibroblast to myofibroblast differentiation via a potential negative feedback loop between CDCP1 expression and TGFβ1 stimulation.

INTRODUCTION

Fibroblasts are the main producers of interstitial extracellular matrix (ECM) which consists of a large number of different macromolecules, including collagens, elastin, large and microfibril-associated glycoproteins, and proteoglycans (4, 10, 14, 22, 31, 47). Fibroblasts play an important role in various cellular responses, including cell proliferation, migration, and adhesion, and are essential for the wound healing process. In the lung, microinjuries to the bronchial and/or alveolar epithelium lead to the release of growth factors, such as transforming growth factor-beta 1 (TGFβ1) resulting in the activation of fibroblasts and their subsequent differentiation into myofibroblasts. On a cellular level, these pathological changes mark the onset of fibrogenic diseases, which lead to loss of respiratory function and finally to death in case of pulmonary fibrosis. Myofibroblasts, which are cellular hallmarks of fibrogenic diseases, are characterized by an increased ECM deposition and expression of alpha smooth muscle actin (αSMA). These functional changes are largely regulated by canonical TGFβ1 signaling and the phosphorylation of Smad3 (17, 20, 37). While the effects of TGFβ1 stimulation on intracellular mediators and downstream targets have been extensively characterized, relatively little information is known on how TGFβ1 regulates cell surface proteins. To this end, we recently performed a cell-surface proteome analysis of lung fibroblasts in the absence/presence of TGFβ1, which identified CDCP1 as one of the top downregulated proteins by TGFβ1 (16).

Cub domain containing protein 1 (CDCP1) is a cell surface glycoprotein expressed in various cell types, including lung epithelial cells, hepatocytes, and hematopoietic progenitor cells (3, 18, 41). Enhanced CDCP1 expression correlates with poor prognosis in patients with various cancers such as lung adenocarcinoma, breast, or pancreas cancer (30, 40, 48). CDCP1 has been implicated in the regulation of tumor invasion and metastasis via interacting with specific molecules such as Src, and PKCδ (30, 36, 48). Additionally, phosphorylated CDCP1 has been

shown to couple with integrin β1, which induces intracellular FAK/PI3K-mediated Akt signaling pathway, and by which cancer cells gain their motility and survival phenotype (5).

In the present study, we investigated the expression and sub-cellular localization of CDCP1 in human lung fibroblasts and further analyzed the functional impact of TGFβ1 on CDCP1 expression and function. We report that TGFβ1 downregulates CDCP1 expression in a time-dependent manner, and that this effect is a combined effect on mRNA and protein levels and may be regulated via ubiquitin-independent proteasomal degradation of CDCP1 (12). Silencing of CDCP1 strongly increased the phosphorylation of Smad3 in the presence of TGFβ1. In functional studies, we observed that depletion of CDCP1 resulted in an increased cell adhesion of primary human lung fibroblasts, which was, however, reliant on TGFβ1. Interestingly, CDCP1-depleted cells displayed a significantly elevated expression of the fibrogenic myofibroblast markers collagen V, and αSMA, and further augmented the effect of TGFβ1 on collagen III, collagen V, and αSMA protein expression. Importantly, CDCP1 was hardly detectable in αSMA-positive myofibroblasts in fibroblastic foci of the fibrotic lung, but strongly enriched in interstitial fibroblasts of the healthy lung. Our data thus show that CDCP1 is a novel negative regulator of TGFβ signaling in fibroblast-to-myofibroblast differentiation via a potential CDCP1/TGFβ1 cross-talk.

MATERIALS AND METHODS

Cell culture and treatment

Primary human lung fibroblasts (phLFs) were isolated from lung tissue derived from lung explants or tumor-free areas of lung resections and further cultured as previously described (43). The study was approved by the local ethics committee of the LMU München (333-10, removal-request 454-12). All experiments were performed with phLFs between passages 5-6. For the experimental procedures, cells were seeded in Dulbecco's modified Eagle's medium: Nutrient

mixture F-12 (DMEM/F-12) supplemented with 20% fetal bovine serum (FBS) and 100 U/ml Penicillin/Streptomycin. phLFs were synchronized 24 h prior the treatment with media containing 0.5 % FBS and antibiotics. Cells were stimulated with 1 ng/ml human recombinant TGFβ1 (R&D System, Minneapolis, USA) every 24 h in starvation media for 48 h if not indicated differently. The inhibitor studies were performed as indicated, using 10 µM SB431542 (1614, Tocris Bioscience, Bristol, UK), 6 µM Sis3 (5291, Tocris Bioscience, Bristol, UK), 10 µM UO126 (1144, Tocris Bioscience, Bristol, UK), 0.05 – 1 µM SCH79797 (1592, Tocris Bioscience, Bristol, UK), 0.1 – 10 µM FSLLRY-NH2 (4751, Tocris Bioscience, Bristol, UK), 0.1 – 10 µM GM6001 (S7157, Selleckchem, Munich, Germany), 1-10 nM Bortezomib (101371, Millennium, Takeda), and 1-10 nM Bafilomycin A1 (B1793, Sigma Aldrich, Munich, Germany). Cells were stimulated with single inhibitors together with 1 ng/ml TGFβ1 every 24 h in the starvation media for 48 h if not indicated differently. Cells were harvested with 0.25% Trypsin-EDTA (25200-056, Gibco).

CDCP1 siRNA-mediated silencing

The siRNA-mediated CDCP1 knockdown was performed as previously described (28). Briefly, phLFs were reverse transfected with 2 nM or 10 nM *Silencer*® Select CDCP1 siRNA (s35060, Ambion, ThermoFisher Scientific, Carlsbad, USA) or 10 nM scrambled *Silencer*® Negative control No. 1 siRNA (AM4611, Ambion, ThermoFisher Scientific, Carlsbad, USA) in Lipofectamine® RNAiMax transfection reagent (13778-150, ThermoFisher Scientific, Carlsbad, USA) as indicated followed by 1 ng/ml TGFβ1 treatment for 48 h if not indicated differently.

Immunofluorescent staining

Cultured phLFs were seeded in a 96-well plate (BD Falcon) or a 24-well plate (µ-Plate 24 Well, Ibidi, Planegg/Martinsried, Germany). Subconfluent cells were fixed either with 4 % PFA in PBS for 15 min or ice-cold methanol for 90 s, and blocked with PBS containing 5 % BSA (A3059-

500G, Sigma Aldrich, Munich, Germany) for 30 min at room temperature (RT). For trypsinization, cells cultured in a 24-well plate (µ-Plate 24 Well, Ibidi, Planegg/Martinsried, Germany) were treated with 0.25 % Trypsin-EDTA (25200-056, Gibco), subsequently fixed and immunostained as described above. Cells were incubated with primary antibody against human CDCP1/CD318 (1:100, PA5-17245, ThermoFisher Scientific), anti-human CD90 (Thy-1) (1:100, 14-9090-82, eBioscience), α-smooth muscle actin (αSMA) (1:5000, A5228, Sigma) (45) at RT for 1 h or overnight at 4°C followed by incubation with fluorescently-labeled anti-rabbit AlexaFluor 568 (1:250, A11011, Invitrogen) and anti-mouse AlexaFluor 488 (1:250, A11001, Invitrogen) secondary antibody. Moreover, Vybrant CFDA Cell Tracer Kit (V12883, ThermoFisher Scientific) was used for intracellular staining of trypsinized cells according to the manufacturer's instructions. DAPI staining was used to visualize cell nuclei. Fluorescent microscopy was performed using an LSM710 laser-scanning system containing an inverted AxioObserver.Z1 stand (Carl Zeiss, Munich, Germany) and images were analyzed using the ZEN 2010 software (Carl Zeiss).

Immunofluorescent staining of tissue sections

The paraffin-embedded donor or IFP tissue sections were placed at 60°C overnight followed by tissue deparaffinization using a Microm HMS 740 Robot-Stainer (ThermoFisher Scientific). Slides were automatically transferred and incubated twice in xylene bath (5 min each), followed by incubation twice in 100 % EtOH (2 min each), and once in 90 % EtOH (1 min), 80 % EtOH (1 min), 70 % EtOH (1 min), and deionized water (1 min) at RT. Sections were placed immediately into R-Universal buffer (Aptum Biologics, Southamptom, UK) for antigen retrieval in a decloacking chamber (2100 Retrieval, Aptum Biologics, Southamptom, UK) for 20 min. Afterwards, slides were washed three times in Tris buffer (0.5 M Tris, 1.5 M NaCl, pH 6.8) and blocked for 1 h at RT using 5 % BSA in PBS. Tissue slides were incubated with primary

antibodies against human CDCP1/CD318 (1:100, PA5-17245, ThermoFisher Scientific) and α-smooth muscle actin (αSMA) (1:5000, A5228, Sigma) (43) in a wet chamber overnight at 4°C followed by secondary antibody incubation with fluorescently-labeled anti-rabbit AlexaFluor 568 (IgG-A568, 1:250, A11011, Invitrogen) and anti-mouse AlexaFluor 488 (IgG-A488, 1:250, A11001, Invitrogen) in a wet chamber for 1 h at RT. Slides were washed three times with Tris buffer and nuclei counterstained with DAPI for 10 min at RT. Finally, slides were covered with Fluorescent Mounting Medium (Dako, Hamburg, Germany) and visualized using an Axio Imager Microscope (Carl Zeiss, Germany).

RNA isolation and Quantitative Real Time Polymerase Chain Reaction (qRT-PCR)

RNA extraction from phLFs was performed using peqGold RNA isolation kit (Peqlab, Erlangen, Germany) according to the manufacturer's instructions. Subsequently, 1µg of isolated RNA was reverse transcribed in a 40 µL reaction mix using M-MLV reverse transcriptase (Promega, Mannheim, Germany) according to the manufacturer's protocol (Life Technologies). Quantitative Real Time PCR (qRT-PCR) was performed using SYBR Green PCR master mix (Roche Applied Science) and the following primers: CDCP1_fw: TTCAGCATTGCAAACCGCTC, CDCP1_rev: ATCAGGGTTGCTGAGCCTTC, ACTA_fw: CGAGATCTCACTGACTACCTCATGA, ACTA_rev: AGAGCTACATAACACAGTTTCTCCTTGA, and for data standardization, human HPRT_fw: AAG GAC CCC ACG AAG TGT TG, HPRT_rev: GGC TTT GTA TTT TGC TTT TCC A. All qRT-PCR reactions were performed in triplicates. Data are presented as -ΔCt values.

FACS analysis

Cells were washed and resuspended in FACS buffer (PBS, 2% FBS, 2 mM EDTA). Subsequently, 2.5 x 10^5 cells per one test were stained with APC-conjugated CDCP1 antibody

(324008, BioLegend. San Diego, USA), and corresponding isotype control (APC mouse IgG2b, BioLegend, San Diego, USA) in the same concentration for 20 min at 4°C. Cells were washed with FACS buffer, and 350 µl of cell suspension was used for the measurement with a FACS LSRII (BD). Data were analyzed using FlowJo software version 9.6.4. Number of positive cells and median fluorescence intensity were determined and calculated as previously described (16).

Western immunoblotting

Cells were lysed in RIPA buffer (50 mM Tris/HCl, pH 7.6, 150 mM NaCl, 1 % Nonidet P-40, 0.5 % sodium deoxycholate, and 0.1 % SDS) as previously described (16). Protein concentration was quantified using the Pierce BCA Protein Assay Kit (10056623, ThermoFisher Scientific). 25 µg of total protein lysate was loaded on 7.5% or 10% SDS-polyacridamide gels, separated, transferred, and detected by WB as previously described (28). Membranes were incubated overnight at 4°C with following antibodies against CDCP1 (1:1000, 4115, Cell Signaling), αSMA (1:1000, A5228, Sigma Aldrich) (45), phospho anti-Smad3 (S423+S425) (1:1000, ab52903, Abcam) (43), anti-Smad3 (1:1000, ab28379, Abcam) (43), Erk1/2 (phospho44/42) (1:1000, 9101, Cell Signaling) (23), Erk1 (1:1000, 554100, BD) (23), Erk2 (1:1000, 610103, BD) (25), Lys^{48}-specific ubiquitin (1:1000, 05-1307, Merck Millipore) (39), LC3B (D11) XP (1:1000, 3868, Cell Signaling) (33), Collagen Type I (1:5000, 600-401-103-0.1, Rockland) (23), Collagen Type III (1:5000, 600-401-105-0.5, Rockland) (23), Collagen V (Coll5A1) (1:1000, sc-20648, Santa Cruz) (43), Fibronectin (1:500, sc-9068, Santa Cruz) (43). For detection, the HRP-linked anti-rabbit (1:25000, NA934, GE Healthcare) and anti-mouse (1:25000, NA931, GE Healthcare) antibodies were used. HRP-conjugated β-actin (1:25000, A3854-200UL, Sigma Aldrich) was used as loading control. Proteins were visualized by autoradiography and normalized to β-actin if not indicated differently.

Immunoprecipitation

Cells were seeded (1.4 x 10^4 per cm^2) and stimulated with TGFβ1 (1 ng/ml), Bortezomib (10 nM), or in combination every 24 h for a total of 48 h and lysed in RIPA buffer as described above. Twenty % of the total lysate was taken as input control for immunoblotting and the leftover used for immunoprecipitation. First, a preclearing step of the lysate was performed by incubating with 75 µL of equilibrated magnetic Dynabeads™ Protein A (10001D, Invitrogen) for 1 h at 4°C while rotating. Subsequently, 0.4 µg of CDCP1 antibody (4115, Cell Signaling) (32) or respective IgG control (VEC-I-1000, Biozol Diagnostica, Eching, Germany) was incubated with total protein lysate for 1 h on ice. 45 µL of equilibrate magnetic beads were added to the lysate for overnight incubation at 4°C while rotating. Beads were washed three times with ice-cold NP-40 buffer (150 mM NaCl, 1% Igepal (NP-40), 50 mM Tris/HCl ph 8.0) under rotating at 4°C. Laemmli buffer was added to the beads and input sample and further analyzed by immunoblotting.

Smad reporter assay

For the experiment, 3 x 10^4 cells per well were reverse transfected for 24 h with 10 nM siRNA against CDCP1 and corresponding scrambled siRNA as described above. 24 h after siRNA transfection, forward transfection for 6 h was performed with 250 ng/ml of the SMAD signaling luciferase reporter plasmid pGL3-CAGA(9)-luc (7) or pGL4-10 control vector construct (E6651, Promega) using Lipofectamine LTX and PLUS reagent (ThermoFisher Scientific, Carlsbad, USA). Afterwards, cells were incubated in starvation medium overnight, and subsequently treated with 1 ng/ml TGFβ1 as indicated. Next day, cells were lysed and cell lysates were used to determine the luciferase activity using Brethold Tristar LB941 (luciferase reagent: Bright-Glo™ Luciferase Assay System, Promega, Mannheim, Germany). All measurements were performed in quadruplicates.

Cell adhesion assay

The phLFs were reverse transfected and/or treated with TGFβ1 as described above. Subsequently, cells were harvested, and the cell number was determined using a Neubauer counting chamber. Next, 1 x 10^4 cells per well were seeded in a 48-well plate in four technical replicates per condition. Cells were resuspended in fresh 0.5 % FBS starvation media and allowed to attach for 10 min at 37°C and 5 % CO_2. After 10 min, non-adherent cells were removed by washing 1x with PBS. Adherent cells were fixed with 4 % PFA for 15 min at RT, washed two times with PBS, and the nuclei and cytoskeleton of the cells stained with DAPI (1:1500) and Rhodamine Phalloidin (1:300, Life Technologies), respectively, for 1 hour at RT. Each well was imaged with an LSM710 by using an EC Plan-Neofluar DICI 10x/0.3 numerical aperture (NA) objective lens (Carl Zeiss). Images were acquired by an 8x8 tile scan to cover the middle area of each well. Data were transferred and quantified by Imaris (Bitplane) version 8.1.2. software. Spot detection algorithm of Imaris was used to assign a spot for each fluorescent intensity of single nuclei. For the spot analysis, we selected region of interest with the following algorithm: (Algorithm) enable region of interest = false; enable region growing = false; enable tracking = false. (Source channel) source channel index = 1; estimated diameter = 27.7; background subtraction = true. (Classify spots) ''quality'' above 1000. By using Imaris' statistical analysis tool, the total number of spot objects, representing the total number of cells, was determined for each treatment.

Statistical analysis

GraphPad Prism 5 was used for all statistical analysis and results are presented as ± SEM, if not indicated differently. For the statistical analysis, a paired two-tailed student's *t*-test was used, if not stated differently. A value of $p<0.05$ was considered as statistically significant *(*p<0.05; **p<0.01; ***p<0.001)*. All experiments were performed in at least three biological replicates.

RESULTS

CDCP1 is expressed on the surface of primary human lung fibroblasts

Expression of the transmembrane glycoprotein CDCP1 in primary human lung fibroblasts (phLFs) has not been described to date. We here report that CDCP1 is expressed on the cell surface of phLFs in the healthy human lung, as evidenced by co-staining with CD90/Thy-1, a commonly accepted cell surface marker for mesenchymal cells (Figure 1). CDCP1 co-localized with CD90/Thy-1 on the surface of PFA-fixed cellular monolayers (Figure 1B), as well as on the surface of detached and thus spherically shaped lung fibroblasts (Figure 1C). In addition, we labeled trypsinized phLFs with Vybrant® CFDA SE intracellular dye and visualized the surface distribution of CDCP1 via 3-dimensional z-stack sections (Figure 1D) to unequivocally document fibroblast cell-surface expression of CDCP1.

TGFβ1 alters CDCP1 expression in primary human lung fibroblasts

We previously showed in a surface proteome profiling, that after treatment of phLFs with TGFβ1, CDCP1 was found to be among the top 15 downregulated proteins (fold change TGFβ1/non-treated cells= -4.07, *p=0.007*) (16). First, we investigated in the current study whether the downregulation of CDCP1 protein expression by TGFβ1 would be an immediate effect or is time-dependent. To do so, we treated phLFs with TGFβ1 at various time points and observed reduced protein expression levels of CDCP1 after 24 h and an even stronger decrease after 48 h (Figure 2A,B). We further corroborated the decline in CDCP1 mRNA and protein levels upon TGFβ1 treatment by performing five independent treatment experiments and subsequent qRT-PCR (Figure 2C) and immunoblotting analysis (Figure 2D). CDCP1 mRNA levels significantly decreased (p-value < 0.001) upon TGFβ1 treatment for 48 h (Figure 2C). Likewise, densitometric analysis revealed a statistically significant downregulation (p-value < 0.01) of CDCP1 total protein levels after 48 h of TGFβ1 treatment (Figure 2E). Primary human fibroblast

cell lines used responded well to the TGFβ1 treatment, as shown by an increase in αSMA mRNA and protein levels (Figure 2A-E). Furthermore, FACS analysis revealed a significant decrease (p-value < 0.01) in the percentage of CDCP1-positive cells upon TGFβ1 treatment (73.5% ± 14.8) when compared to non-treated cells (85.7% ± 10.0) (Figure 2F,G). A similar result was observed for the median fluorescence intensity (MFI) values, which decreased for CDCP1 among all cells (1559.1 ± 1172.0 to 585.9 ± 351.2) (p-value < 0.05) (Figure 2G).

Decline in CDCP1 protein expression levels by TGFβ1 is independent of SMAD signaling

Next, we wanted to investigate the molecular mechanism by which TGFβ1 downregulates CDCP1 expression and therefore blocked different molecules of canonical and non-canonical TGFβ1 signaling. First, we assessed pSmad3 levels of the canonical TGFβ1 signaling pathway in phLFs in the presence of either SB431542, a specific inhibitor targeting the TGFβ1 receptor Alk5, or Sis3, a specific inhibitor of Smad3 phosphorylation, together with TGFβ1 stimulation for 48 h. Immunoblotting analysis showed a reduced expression of CDCP1 by TGFβ1 alone. Expression levels of CDCP1 still remained low in the cells treated with TGFβ1 together with either SB431542 or Sis3 (Figure 3A,B). Similar low CDCP1 levels were observed when using inhibitors of the non-canonical TGFβ1 pathway that specifically target pErk1/2 (UO126), PAR1, PAR2, and a broad spectrum of matrix metalloproteases including MMP1-3, MMP7-9, MMP12, MMP14, and MMP26 (GM6001) (Figure 3C-F). Taken together, these data indicate that TGFβ1 alters CDCP1 expression by a SMAD independent mechanism.

TGFβ1 decreases CDCP1 expression via ubiquitin-independent proteasomal degradation

Another cellular mechanism altering protein levels is autophagy. We therefore tested if TGFβ1 mediates downregulation of CDCP1 expression via autophagic degradation. Therefore, we treated phLFs with Bafilomycin, an inhibitor of the late phase of autophagy, together with TGFβ1

for 48 h. Subsequently, we evaluated CDCP1 protein expression via immunoblotting. The expression levels of CDCP1 remained decreased in cells treated with Bafilomycin in the presence of TGFβ1 (Figure 4A). Moreover, there was no difference in Smad3 phosphorylation levels between control and Bafilomycin-treated cells in the presence of TGFβ1, indicating a different mechanism, other than autophagy, that is regulating CDCP1's downregulation by TGFβ1 treatment (Figure 4A).

Since the proteasome is one of the main proteolytic systems of the cell, we hypothesized that TGFβ1 drives the decrease of CDCP1 expression via its degradation in the proteasome. In order to examine this hypothesis, we treated lung fibroblasts in a dose-dependent manner with the proteasome inhibitor Bortezomib together with TGFβ1 for 48 h and analyzed CDCP1 protein expression via immunoblotting (Figure 4B). Interestingly, 10 nM of Bortezomib prevented the downregulation of CDCP1 in the presence of TGFβ1 (Figure 4C), suggesting that CDCP1 might be degraded in the proteasome upon TGFβ1 treatment (Figure 4B). To further strengthen this observation, phLFs were treated with 10 nM of Bortezomib for 48 h and the ubiquitination status of CDCP1 in the presence of TGFβ1 analyzed via pulldown experiments using an antibody directed against CDCP1 (Figure 4D). Immunoblotting indicated a high enrichment of CDCP1 via immunoprecipitation, however no ubiquitination of CDCP1 upon treatment was detected (Figure 4D). Importantly, Bortezomib treatment in the presence of TGFβ1 restored expression of CDCP1 already on the mRNA level (Figure 4E). These data indicate that CDCP1 degradation in the proteasome mediated by TGFβ1 might not be due to protein ubiquitination, but via a different yet unknown mechanism. Of note, 10 nM of Bortezomib also constrained the TGFβ1-mediated increase in αSMA protein (Figure 4C) and mRNA (Figure 4E) levels.

The siRNA-mediated knockdown affects cell surface and total protein levels of CDCP1

To further study the functional role of CDCP1 in lung fibroblasts, we performed siRNA-mediated knockdown of CDCP1 at different time points. The surface localization of CDCP1 was monitored by flow cytometry showing a significant decrease (p-value < 0.001) in the percentage of CDCP1 positive cells (85.3 ± 10.0 to 45.7 ± 12.1) after 48 h (Figure 5A,B). Similarly, MFI values were significantly decreased for CDCP1 (p-value < 0.05) among all cells in the knockdown condition (2607.8 ± 2326.2 to 177.5 ± 158.2) (Figure 5B). Western blot analysis exhibited an effective total protein depletion of CDCP1 upon siRNA knockdown after 48 h, and 72 h, whereas αSMA levels increased in the absence of CDCP1 (Figure 5C).

Absence of CDCP1 increases Smad3 phosphorylation in the presence of TGFβ1

To investigate whether CDCP1 modulates TGFβ1 signaling, we performed siRNA-mediated silencing of CDCP1 followed by TGFβ1 treatment for 1 h, 26 h, and 48 h and changes in Smad3 phosphorylation were monitored via immunoblotting. As expected, TGFβ1 led to an increase in Smad3 phosphorylation (Figure 6A-C). Interestingly, silencing of CDCP1 showed an even significantly stronger increase (p-value < 0.05) in pSmad3 levels in a TGFβ1-dependent manner (Figure 6D). To further validate our data, we treated phLFs as described above and performed Smad-signaling luciferase reporter assay using the Smad3-reporter (pGL3-CAGA(9)-luc) plasmid, which contains 12 tandem repeats of the upstream Smad3-binding element from human PAI-1 promoter linked to a viral minimal promoter and a luciferase gene (7), and a pGL4-10 control plasmid. Knockdown of CDCP1 significantly increased (p-value < 0.05) TGFβ1 induced Smad3 promoter activity after 26 h (fold change siCDCP1+ TGFβ1/siScr+TGFβ1=2.0) and 48 h (fold change siCDCP1+ TGFβ1/siScr+TGFβ1=3.1) as shown in Figure 6E,F. Taken together, our data indicate that CDCP1 negatively regulates TGFβ1 signaling in the presence of TGFβ1.

Knockdown of CDCP1 increases cell adhesion in primary human lung fibroblasts

CDCP1 has been shown to play a role in cell adhesion by modulating attachment of certain cancer cell lines to the extracellular matrix (9, 49). Fibroblasts are actively participating in various cellular responses, including cell adhesion (47). We therefore sought to investigate CDCP1's contribution to cell adhesion in phLFs and how this is dependent on TGFβ1. We performed a transient knockdown of CDCP1 followed by TGFβ1 stimulation for 48 h and determined the number of attached cells by using immunofluorescent microscopy. Although depletion of CDCP1 alone did not show a significant increase in the adhesion capacity of phLFs compared to control siRNA-transfected cells, the numbers of attached cells significantly increased (p-value < 0.01) when knockdown of CDCP1 was followed by TGFβ1 stimulation (Figure 7A,B).

Knockdown of CDCP1 increases the protein expression of αSMA and ECM components

It is generally known that TGFβ1 increases the expression of ECM components, such as collagens and fibronectin (20, 34, 50). To investigate a possible impact of CDCP1 on ECM deposition, we treated phLFs with TGFβ1 for 48 h and assessed the protein expression of collagen I, collagen III, collagen V and fibronectin in the presence and absence of CDCP1 (Figure 8A). As expected, expression levels of collagens and fibronectin were found to be elevated after TGFβ1 treatment. Interestingly, CDCP1 knockdown alone led to a significant increase in collagen V protein levels, and strongly enhanced the effect of TGFβ1 on collagen III and collagen V expression (Figure 8A,B). TGFβ1 is also one of the main drivers of fibroblast to myofibroblast differentiation that is accompanied by an increase in αSMA protein expression levels (17, 19). Here, we observed that knockdown of CDCP1 led to an increase in αSMA expression in the presence and absence of TGFβ1, as shown in Figure 8A to C via immunoblotting and immunofluorescent microscopy of phLFs. Moreover, immunofluorescence stainings of IPF tissue sections revealed hardly-detectable expression of CDCP1 in αSMA-

positive interstitial myofibroblasts located in fibroblastic foci, whereas interstitial fibroblasts in sections from donor lungs showed a positive staining for CDCP1, but were negative for αSMA (Figure 4D). Taken together, our data indicate a novel role of CDCP1 in the process of fibroblast to myofibroblast transdifferentiation.

DISCUSSION

In the present study, we show for the first time that CDCP1 is localized to the cell-surface of phLFs, and that TGFβ1 is a strong negative regulator of CDCP1 expression. We suggest that this decline in CDCP1 expression is a result of complex regulatory pathways affecting the mRNA and protein levels of CDCP1, which may be mediated via a non-conventional ubiquitin-independent proteasome pathway. Silencing of CDCP1 by siRNA led to an increase in Smad3 phosphorylation levels in the presence of TGFβ1, and enhanced TGFβ1-mediated cell adhesion capacity of phLFs. Finally, we described for the first time that CDCP1-depleted cells displayed an upregulation in collagen V and αSMA, and further strongly enhanced the effect of TGFβ1 on collagen III, collagen V, and aSMA. Changes in the protein expression of these fibrogenic marker proteins were found to be independent of the canonical and non-canonical TGFβ1 signaling pathway. Moreover, we show that αSMA-negative interstitial lung fibroblasts of healthy lungs express high levels of CDCP1, whereas αSMA-positive myofibroblasts in fibroblastic foci of IPF lungs hardly express detectable CDCP1 levels at all.

CDCP1 is a transmembrane glycoprotein whose protein expression has been described in epithelial cells of lung, colon, and pancreas, liver hepatocytes, primary cultures of foreskin keratinocytes, and hematopoietic cells (1, 2, 6, 18, 41). In this study we confirmed our recent proteome data (16) and showed expression and surface localization of CDCP1 in human lung fibroblasts using qRT-PCR, immunoblotting, immunofluorescent stainings, and FACS. This stands in contrast to findings of Hooper *et al*. reporting that endothelial cells and fibroblasts do

not express CDCP1. Their study, however, was performed with dermal fibroblasts (18). Little is known about upstream regulators of CDCP1. Here, we showed that TGFβ1 downregulates CDCP1 expression on mRNA and protein levels in phLFs (Figure 2). Contrarily, an upregulation of CDCP1 by TGFβ1, BMP4, and HGF on mRNA and protein levels has been described in pancreatic cancer cells (29). This indicates a distinct cellular CDCP1 expression, and regulation by TGFβ1 in different organs and cell types. Interestingly, in our mechanistic study we found for the first time that TGFβ1 potentially induces an ubiquitin-independent degradation of CDCP1 by the proteasome, but is not acting via the canonical Smad3 or MAPK signaling pathways (Figure 3,4). TGFβ1 has previously been reported to induce ubiquitin-mediated proteasome degradation of PTHrP in human hepatocarcinoma cells (26)**.** A similar effect was observed for estrogen receptor alpha (ERα) in breast cancer cell lines, where the proteasome inhibitor MG132 prevented TGFβ1-mediated decrease in ERα total protein levels (35). In our study, we did not detect ubiquitinated CDCP1. An ubiquitin-independent proteasomal degradation of proteins, however, has been described. Kong and colleagues showed that degradation of HIF-1α mediated via the histone deacetylase (HDAC) TSA is ubiquitination independent, as RCC4 cells displayed a lack of HIF-α ubiquitination when using the proteasome inhibitor MG132. Instead, they proposed that inhibition of HDAC-6 leads to the hyperacetylation of HSP90, a HIF-1α chaperone protein which in consequence results in accumulation and further degradation of immature HIF-α/HSP70 complex in the proteasome (24). On the other hand, we observed that TGFβ1 decreased CDCP1 expression already on mRNA levels (Figure 2), and this effect was further inhibited in the presence of Bortezomib (Figure 4). An alternative mechanism of CDCP1's expression regulation by TGFβ1 could be that a positive regulator of CDCP1 transcription is degraded via an ubiquitin-dependent proteasomal pathway following TGFβ1 stimulation. A similar effect was observed by Terme and colleagues for TAL1/SLC, a basic helix-loop-helix transcription factor essential for hematopoietic and endothelial cell differentiation (44). Here, the authors reported that TGFβ1 induces a polyubiquitination, causing a proteasome-mediated

degradation of TAL1/SCL in HeLa and Jurkat cells, leading to a decreased expression of TAL1/SLC in leukemic cells. Additionally, they found that this effect depends on TAL1/SCL phosphorylation by Akt1 which increases association of the oncogene with the E3 ubiquitin ligase CHIP. By now information about CDCP1's transcriptional regulation is scarce. Recently, HIF-2α was introduced as a novel regulator of CDCP1 transcription in MCF10A cells (11). However, it has been reported that TGFβ1 upregulates HIF-2α expression in human mesangial cells (15) indicating that another transcriptional regulator may be involved in this process.

Our data also provide evidence that CDCP1 interferes with TGFβ1 signaling. Knockdown of CDCP1 increased the phosphorylation levels of Smad3 in the presence of TGFβ1 (Figure 6) and importantly, led to an increase in αSMA and collagen V protein expression independent of TGFβ1 (Figure 8). TGFβ1 and its downstream signaling pathway is a major driver of fibroblast to myofibroblast transdifferentiation. The most frequently used cytoskeletal marker for differentiated myofibroblasts is αSMA, which is also expressed by other cell types, such as smooth muscle cells (38). We also showed that αSMA-positive myofibroblasts, that accumulated in fibroblastic foci of IPF lungs, display a very modest CDCP1 expression when compared to non-differentiated interstitial lung fibroblasts in non-diseased conditions, which were found to be strongly positive for CDCP1 and negative for aSMA (Figure 8D). In fibroblasts, αSMA expression is mainly regulated by canonical TGFβ signaling via the phosphorylation of Smad2/3 (13, 27). Additionally, TGFβ1 activates different non-Smad pathways, including MAPK, Rho-like GTPase, and PI3K/Akt signaling pathways (8, 50). There is limited information regarding a possible CDCP1-mediated signaling pathway. Recently, Casar *et al*. reported that extracellular cleavage of 135 kDa full-length CDCP1 by serine proteases generates a short 70 kDa CDCP1 fragment, which becomes activated by intracellular interaction of CDCP1 with pSrc and pPKCδ. Activated CDCP1 couples with integrin β1 and forms a CDCP1-integrin β1 complex on the cell surface. This interaction further augments intracellular phosphorylation of integrin-associated focal

adhesion kinase (FAK) leading to activation of PI3K-Akt signaling pathway by which cancer cells lose their adhesion properties and gain a metastatic phenotype (5).

We also showed that CDCP1 plays a role in TGFβ1-mediated cell adhesion of phLFs. While absence of CDCP1 did not significantly increase cell adhesion, the numbers of attached cells significantly increased in the presence of TGFβ1 (Figure 7). To our knowledge this finding has not been reported to date. Several studies, however, have shown that CDCP1 regulates the adhesion of cancer cell lines to the ECM (2, 9, 46, 49). Uekita *et al.* investigated the effect of CDCP1 expression on cell-ECM adhesion in scirrhous gastric cancer cells observing an increased number of attached cells on fibronectin, but not on collagen type 1 or Matrigel surfaces in the absence of CDCP1 (46). Additionally, Spassov *et al*. showed that phosphorylation of CDCP1 results in a detachment of epithelial cells from fibronectin-coated coverslips. On the other hand, CDCP1 dephosphorylation is linked with the re-adherence of cells to the ECM (42).

Activated myofibroblasts play a key role in tissue remodeling by producing, secreting and depositing an excessive number of ECM components, such as collagens and fibronectin. Interestingly, Miyazawa and colleagues observed that loss of CDCP1 expression suppressed ECM degradation through decreased secretion of MMP-9 proteases in pancreatic cancer cell lines (30). In our study, we also detected a negative effect of CDCP1 on ECM expression under both, basal and TGFβ1-stimulated conditions (Figure 8). In particular, CDCP1 depletion significantly enhanced a TGFβ1-mediated increase of collagen III and collagen V in phLFs (Figure 8A,B). The expression of both, collagen III and collagen V, is highly elevated in IPF where they actively contribute to the collagen-remodeling processes during ongoing fibrosis (21, 34).

In sum, our study highlights that TGFβ1 not only regulates the expression of intracellular proteins, such as αSMA in myofibroblasts, but also alters the expression and function of surface

proteins, as exemplified here for CDCP1. There is still limited information regarding CDCP1 signaling and its impact on cellular function. Therefore, further work is required to identify the mechanism behind CDCP1 and TGFβ1 pathway interaction in lung fibroblasts, especially in the context of ligand(s) and interaction partners of CDCP1 taking part in a potential cross-talk with TGFβ signaling. This will shed new light on the precise role of transmembrane proteins and CDCP1, in particular in processes relevant to wound healing and their pathophysiological consequences for scarring and fibrotic disease.

GRANTS

This study was funded by the Helmholtz Association (BMBF) and the German Center for Lung Research (DZL).

DISCLOSURES

The authors Nina Noskovičová, Dr. Katharina Heinzelmann, Dr. Gerald Burgstaller, and Dr. Jürgen Behr declare that they have no conflicts of interest with the contents of this article. Dr. Oliver Eickelberg reports consulting fees from MorphoSys AG, Novartis Pharma AG, Galapagos NV, and Lanthio Pharma B.V., outside of the submitted work.

AUTHOR CONTRIBUTIONS

N.N., K.H., G.B., J.B., and O.E. designed the study. N.N., K.H., and G.B. performed experiments. N.N., K.H., G.B., and O.E. acquired, analyzed, discussed, and interpreted data. N.N. drafted the manuscript. K.H., G.B., and O.E. critically reviewed the manuscript.

ACKNOWLEDGEMENTS

We thank the CPC-M BioArchive for kindly providing human material for this work. We are very grateful for the contribution of the clinical and surgical team (Prof. Rudolf Hatz, Dr. Michael Lindner, Dr. Hauke Winter, Dr. Gerhard Preissler) of the University Hospital Munich for providing tissue to the BioArchive CPC-M. We are also grateful to Dibora Tibebu and Heike Hoffmann for excellent technical support and to all members of the Eickelberg lab, specifically Dr. Claudia Staab-Weijnitz for intensive discussion. We also thank Dr. Silke Meiners and Vanessa Welk for valuable help and discussion of proteasome data.

REFERENCES

1. **Alvares SM**, **Dunn CA**, **Brown TA**, **Wayner EE**, **Carter WG**. The role of membrane microdomains in transmembrane signaling through the epithelial glycoprotein Gp140/CDCP1. *Biochim Biophys Acta* 1780: 486–96, 2008.
2. **Brown TA**, **Yang TM**, **Zaitsevskaia T**, **Xia Y**, **Dunn CA**, **Sigle RO**, **Knudsen B**, **Carter WG**. Adhesion or plasmin regulates tyrosine phosphorylation of a novel membrane glycoprotein p80/gp140/CUB domain-containing protein 1 in epithelia. *J Biol Chem* 279: 14772–83, 2004.
3. **Buhring H-J**, **Kuçi S**, **Conze T**, **Rathke G**, **Bartolović K**, **Grünebach F**, **Scherl-Mostageer M**, **Brümmendorf TH**, **Schweifer N**, **Lammers R**. CDCP1 Identifies a Broad Spectrum of Normal and Malignant Stem/Progenitor Cell Subsets of Hematopoietic and Nonhematopoietic Origin. *Stem Cells* 22: 334–343, 2004.
4. **Burgstaller G**, **Oehrle B**, **Gerckens M**, **White ES**, **Schiller HB**, **Eickelberg O**. The instructive extracellular matrix of the lung: basic composition and alterations in chronic lung disease [Online]. *Eur Respir J* 50, 2017. http://erj.ersjournals.com/content/50/1/1601805.long [17 Aug. 2017].
5. **Casar B**, **Rimann I**, **Kato H**, **Shattil SJ**, **Quigley JP**, **Deryugina EI**. In vivo cleaved CDCP1 promotes early tumor dissemination via complexing with activated β1 integrin and induction of FAK/PI3K/Akt motility signaling. *Oncogene* 33: 255–68, 2014.
6. **Conze T**, **Lammers R**, **Kuci S**, **Scherl-Mostageer M**, **Schweifer N**, **Kanz L**, **Buhring H-J**. CDCP1 is a novel marker for hematopoietic stem cells. [Online]. *Ann N Y Acad Sci* 996: 222–6, 2003. http://www.ncbi.nlm.nih.gov/pubmed/12799299 [24 Feb. 2016].
7. **Dennler S**, **Itoh S**, **Vivien D**, **ten Dijke P**, **Huet S**, **Gauthier JM**. Direct binding of Smad3 and Smad4 to critical TGF beta-inducible elements in the promoter of human plasminogen activator inhibitor-type 1 gene. *EMBO J* 17: 3091–100, 1998.
8. **Derynck R**, **Zhang YE**. Smad-dependent and Smad-independent pathways in TGF-beta family signalling. *Nature* 425: 577–84, 2003.
9. **Deryugina EI**, **Conn EM**, **Wortmann A**, **Partridge JJ**, **Kupriyanova TA**, **Ardi VC**, **Hooper JD**, **Quigley JP**. Functional role of cell surface CUB domain-containing protein 1 in tumor cell dissemination. *Mol Cancer Res* 7: 1197–211, 2009.
10. **Dunsmore SE**, **Rannels DE**. Extracellular matrix biology in the lung. [Online]. *Am J Physiol* 270: L3-27, 1996. http://www.ncbi.nlm.nih.gov/pubmed/8772523 [27 Feb. 2017].
11. **Emerling BM**, **Benes CH**, **Poulogiannis G**, **Bell EL**, **Courtney K**, **Liu H**, **Choo-Wing R**, **Bellinger G**, **Tsukazawa KS**, **Brown V**, **Signoretti S**, **Soltoff SP**, **Cantley LC**. Identification of CDCP1 as a hypoxia-inducible factor 2α (HIF-2α) target gene that is associated with survival in clear cell renal cell carcinoma patients. *Proc Natl Acad Sci U S A* 110: 3483–8, 2013.
12. **Erales J**, **Coffino P**. Ubiquitin-independent proteasomal degradation. *Biochim Biophys Acta* 1843: 216–21, 2014.
13. **Feng X-H**, **Derynck R**. SPECIFICITY AND VERSATILITY IN TGF-β SIGNALING THROUGH

SMADS. *Annu Rev Cell Dev Biol* 21: 659–693, 2005.

14. **Frantz C**, **Stewart KM**, **Weaver VM**. The extracellular matrix at a glance. *J Cell Sci* 123: 4195–200, 2010.
15. **Hanna C**, **Hubchak SC**, **Liang X**, **Rozen-Zvi B**, **Schumacker PT**, **Hayashida T**, **Schnaper HW**. Hypoxia-inducible factor-2α and TGF-β signaling interact to promote normoxic glomerular fibrogenesis. *Am J Physiol Renal Physiol* 305: F1323-31, 2013.
16. **Heinzelmann K**, **Noskovičová N**, **Merl-Pham J**, **Preissler G**, **Winter H**, **Lindner M**, **Hatz R**, **Hauck SM**, **Behr J**, **Eickelberg O**. Surface proteome analysis identifies platelet derived growth factor receptor-alpha as a critical mediator of transforming growth factor-beta-induced collagen secretion. *Int J Biochem Cell Biol* 74: 44–59, 2016.
17. **Hinz B**, **Phan SH**, **Thannickal VJ**, **Galli A**, **Bochaton-Piallat M-L**, **Gabbiani G**. The Myofibroblast. *Am J Pathol* 170: 1807–1816, 2007.
18. **Hooper JD**, **Zijlstra A**, **Aimes RT**, **Liang H**, **Claassen GF**, **Tarin D**, **Testa JE**, **Quigley JP**. Subtractive immunization using highly metastatic human tumor cells identifies SIMA135/CDCP1, a 135 kDa cell surface phosphorylated glycoprotein antigen. *Oncogene* 22: 1783–94, 2003.
19. **Hu B**, **Wu Z**, **Phan SH**. Smad3 Mediates Transforming Growth Factor-β–Induced α-Smooth Muscle Actin Expression. *Am J Respir Cell Mol Biol* 29: 397–404, 2003.
20. **Kendall RT**, **Feghali-Bostwick CA**. Fibroblasts in fibrosis: novel roles and mediators. *Front Pharmacol* 5: 123, 2014.
21. **Kenyon NJ**, **Ward RW**, **McGrew G**, **Last JA**. TGF-beta1 causes airway fibrosis and increased collagen I and III mRNA in mice. *Thorax* 58: 772–7, 2003.
22. **Klingberg F**, **Hinz B**, **White ES**. The myofibroblast matrix: implications for tissue repair and fibrosis. *J Pathol* 229: 298–309, 2013.
23. **Knüppel L**, **Ishikawa Y**, **Aichler M**, **Heinzelmann K**, **Hatz R**, **Behr J**, **Walch A**, **Bächinger HP**, **Eickelberg O**, **Staab-Weijnitz CA**. A Novel Antifibrotic Mechanism of Nintedanib and Pirfenidone. Inhibition of Collagen Fibril Assembly. *Am J Respir Cell Mol Biol* 57: 77–90, 2017.
24. **Kong X**, **Lin Z**, **Liang D**, **Fath D**, **Sang N**, **Caro J**. Histone Deacetylase Inhibitors Induce VHL and Ubiquitin-Independent Proteasomal Degradation of Hypoxia-Inducible Factor 1. *Mol Cell Biol* 26: 2019–2028, 2006.
25. **Lefloch R**, **Pouysségur J**, **Lenormand P**. Single and combined silencing of ERK1 and ERK2 reveals their positive contribution to growth signaling depending on their expression levels. *Mol Cell Biol* 28: 511–27, 2008.
26. **Li H**, **He G**, **Yao H**, **Song L**, **Zeng L**, **Peng X**, **Rosol TJ**, **Deng X**. TGF-β Induces Degradation of PTHrP Through Ubiquitin-Proteasome System in Hepatocellular Carcinoma. *J Cancer* 6: 511–8, 2015.
27. **Massagué J**, **Seoane J**, **Wotton D**. Smad transcription factors. *Genes Dev* 19: 2783–810, 2005.
28. **Mise N**, **Savai R**, **Yu H**, **Schwarz J**, **Kaminski N**, **Eickelberg O**. Zyxin is a transforming growth factor-β (TGF-β)/Smad3 target gene that regulates lung cancer cell motility via integrin α5β1. *J Biol*

Chem 287: 31393–405, 2012.

29. **Miura S**, **Hamada S**, **Masamune A**, **Satoh K**, **Shimosegawa T**. CUB-domain containing protein 1 represses the epithelial phenotype of pancreatic cancer cells. *Exp Cell Res* 321: 209–18, 2014.

30. **Miyazawa Y**, **Uekita T**, **Hiraoka N**, **Fujii S**, **Kosuge T**, **Kanai Y**, **Nojima Y**, **Sakai R**. CUB domain-containing protein 1, a prognostic factor for human pancreatic cancers, promotes cell migration and extracellular matrix degradation. *Cancer Res* 70: 5136–46, 2010.

31. **Mouw JK**, **Ou G**, **Weaver VM**. Extracellular matrix assembly: a multiscale deconstruction. *Nat Rev Mol Cell Biol* 15: 771–85, 2014.

32. **Nakashima K**, **Uekita T**, **Yano S**, **Kikuchi J-I**, **Nakanishi R**, **Sakamoto N**, **Fukumoto K**, **Nomoto A**, **Kawamoto K**, **Shibahara T**, **Yamaguchi H**, **Sakai R**. Novel small molecule inhibiting CDCP1-PKCδ pathway reduces tumor metastasis and proliferation. *Cancer Sci* 108: 1049–1057, 2017.

33. **Nho RS**, **Hergert P**. IPF fibroblasts are desensitized to type I collagen matrix-induced cell death by suppressing low autophagy via aberrant Akt/mTOR kinases. *PLoS One* 9: e94616, 2014.

34. **Parra ER**, **Teodoro WR**, **Velosa APP**, **de Oliveira CC**, **Yoshinari NH**, **Capelozzi VL**. Interstitial and vascular type V collagen morphologic disorganization in usual interstitial pneumonia. *J Histochem Cytochem* 54: 1315–25, 2006.

35. **Petrel TA**, **Brueggemeier RW**. Increased proteasome-dependent degradation of estrogen receptor-alpha by TGF-beta1 in breast cancer cell lines. *J Cell Biochem* 88: 181–90, 2003.

36. **Razorenova O V**, **Finger EC**, **Colavitti R**, **Chernikova SB**, **Boiko AD**, **Chan CKF**, **Krieg A**, **Bedogni B**, **LaGory E**, **Weissman IL**, **Broome-Powell M**, **Giaccia AJ**. VHL loss in renal cell carcinoma leads to up-regulation of CUB domain-containing protein 1 to stimulate PKC{delta}-driven migration. *Proc Natl Acad Sci U S A* 108: 1931–6, 2011.

37. **Sakai N**, **Tager AM**. Fibrosis of two: Epithelial cell-fibroblast interactions in pulmonary fibrosis. *Biochim Biophys Acta* 1832: 911–21, 2013.

38. **Sartore S**, **Chiavegato A**, **Faggin E**, **Franch R**, **Puato M**, **Ausoni S**, **Pauletto P**. Contribution of adventitial fibroblasts to neointima formation and vascular remodeling: from innocent bystander to active participant. [Online]. *Circ Res* 89: 1111–21, 2001. http://www.ncbi.nlm.nih.gov/pubmed/11739275 [24 Nov. 2016].

39. **Semren N**, **Welk V**, **Korfei M**, **Keller IE**, **Fernandez IE**, **Adler H**, **Günther A**, **Eickelberg O**, **Meiners S**. Regulation of 26S Proteasome Activity in Pulmonary Fibrosis. *Am J Respir Crit Care Med* 192: 1089–1101, 2015.

40. **Scherl-Mostageer M**, **Sommergruber W**, **Abseher R**, **Hauptmann R**, **Ambros P**, **Schweifer N**. Identification of a novel gene, CDCP1, overexpressed in human colorectal cancer. [Online]. *Oncogene* 20: 4402–8, 2001. http://www.ncbi.nlm.nih.gov/pubmed/11466621 [23 Nov. 2016].

41. **Siva AC**, **Wild MA**, **Kirkland RE**, **Nolan MJ**, **Lin B**, **Maruyama T**, **Yantiri-Wernimont F**, **Frederickson S**, **Bowdish KS**, **Xin H**. Targeting CUB domain-containing protein 1 with a monoclonal antibody inhibits metastasis in a prostate cancer model. *Cancer Res* 68: 3759–66, 2008.

42. **Spassov DS**, **Baehner FL**, **Wong CH**, **McDonough S**, **Moasser MM**. The transmembrane src substrate Trask is an epithelial protein that signals during anchorage deprivation. *Am J Pathol* 174: 1756–65, 2009.
43. **Staab-Weijnitz CA**, **Fernandez IE**, **Knüppel L**, **Maul J**, **Heinzelmann K**, **Juan-Guardela BM**, **Hennen E**, **Preissler G**, **Winter H**, **Neurohr C**, **Hatz R**, **Lindner M**, **Behr J**, **Kaminski N**, **Eickelberg O**. FK506-Binding Protein 10, a Potential Novel Drug Target for Idiopathic Pulmonary Fibrosis. *Am J Respir Crit Care Med* 192: 455–67, 2015.
44. **Terme J-M**, **Lhermitte L**, **Asnafi V**, **Jalinot P**. TGF- induces degradation of TAL1/SCL by the ubiquitin-proteasome pathway through AKT-mediated phosphorylation. *Blood* 113: 6695–6698, 2009.
45. **Torr EE**, **Ngam CR**, **Bernau K**, **Tomasini-Johansson B**, **Acton B**, **Sandbo N**. Myofibroblasts exhibit enhanced fibronectin assembly that is intrinsic to their contractile phenotype. *J Biol Chem* 290: 6951–61, 2015.
46. **Uekita T**, **Tanaka M**, **Takigahira M**, **Miyazawa Y**, **Nakanishi Y**, **Kanai Y**, **Yanagihara K**, **Sakai R**. CUB-Domain-Containing Protein 1 Regulates Peritoneal Dissemination of Gastric Scirrhous Carcinoma. *Am J Pathol* 172: 1729–1739, 2008.
47. **White ES**. Lung extracellular matrix and fibroblast function. *Ann Am Thorac Soc* 12 Suppl 1: S30-3, 2015.
48. **Wong CH**, **Baehner FL**, **Spassov DS**, **Ahuja D**, **Wang D**, **Hann B**, **Blair J**, **Shokat K**, **Welm AL**, **Moasser MM**. Phosphorylation of the SRC epithelial substrate Trask is tightly regulated in normal epithelia but widespread in many human epithelial cancers. *Clin Cancer Res* 15: 2311–22, 2009.
49. **Xia Y**, **Gil SG**, **Carter WG**. Anchorage mediated by integrin alpha6beta4 to laminin 5 (epiligrin) regulates tyrosine phosphorylation of a membrane-associated 80-kD protein. [Online]. *J Cell Biol* 132: 727–40, 1996. http://www.pubmedcentral.nih.gov/articlerender.fcgi?artid=2199869&tool=pmcentrez&rendertype=abstract [24 Nov. 2016].
50. **Zhang YE**. Non-Smad pathways in TGF-beta signaling. *Cell Res* 19: 128–39, 2009.

660 **FIGURE LEGENDS**

661 **Figure 1. CDCP1 is localized to the surface of phLFs.** (A) Confocal fluorescence microscopy
662 of phLFs stained with antibodies to human CDCP1 (red) or (B) stained with antibodies to human
663 CDCP1 (red) and human CD90 (Thy-1) (green). Nuclei were visualized with DAPI (blue). (C)
664 Confocal fluorescence microscopy of phLFs immunostained for CDCP1 (red) and CD90 (green),
665 showing surface localization of CDCP1 and CD90. Nuclei were visualized with DAPI (blue). (D)
666 Orthoview of a confocal z-stack displaying trypsinized phLFs that were labeled with Vybrant
667 CFDA dye (green) and immunofluorescently labelled for CDCP1 (red). Nuclei were visualized
668 with DAPI (blue). Note that CDCP1 localizes to the surface of the displayed cell and the green
669 Vybrant CFDA dye only labels the cell's cytoplasm. For all images, one representative image of
670 three technical replicates from three biological experiments is shown (n=3). *Scale bars*: (A) 200
671 µm, (B) and (D) 20 µm, (C) 10 µm.
672
673 **Figure 2. CDCP1 expression is altered by TGFβ1 in phLFs.** PhLFs were treated over time in
674 the presence/absence of 1 ng/ml TGFβ1 and the expression changes of CDCP1 and αSMA
675 analyzed via immunoblot (A). Shown is one representative Western blot of four performed
676 biological experiments (n=4) with densitometric quantification of CDCP1/β-actin and αSMA/β-
677 actin ratio in (B). Quantitative RT-PCR (C) and immunoblot (D) analysis of CDCP1 and αSMA
678 expression from five different fibroblast cell lines (n=5) treated with TGFβ1 for 48 h. (E)
679 Densitometric quantification of CDCP1 and αSMA expression from (D) normalized to β-actin. (F)
680 The percentage of CDCP1 positive cells in the presence/absence of TGFβ1 was determined by
681 FACS. Histogram and dot blot are shown with the isotype control labeled in red and the CDCP1-
682 positive population in blue. (G) *Left graph*: Percentage of CDCP1 positive cells from (E) shown
683 as a summary of seven independent experiments (n=7). *Right graph*: The respective median
684 fluorescence intensity (MFI) values (ΔMFI) calculated by the subtraction of the isotype MFI

values shown as a summary from seven independent experiments (n=7). For each experiment, data are presented as ± SEM. Statistical analysis: Paired two-tailed *t-test.* ***p<0.001, **p<0.01, *p<0.05. wo = non-treated cells.

Figure 3. TGFβ1 decreases CDCP1 expression via a Smad-independent signaling pathway. Immunoblotting of whole cell lysates obtained from phLFs treated with 1 ng/ml TGFβ1 together with specific inhibitors targeting (A) Alk5 receptor (SB431542), (B) phosphorylated Smad3 (Sis3), (C) pErk1/2 (UO126), (D) PAR1, (E) PAR2, and various MMPs (GM6001) every 24 h for a total 48 h treatment period. Cell lysates were probed for CDCP1, phospho anti-Smad3 (S423+S425), anti-Smad3, phospho-p44/42 MAPK (Erk1/2) (Thr202/Tyr204), anti-Erk1, anti-Erk2, and αSMA. In each case, β-actin was used as a loading control. Untreated samples are indicated by "wo". Each blot is representative for three independent experiments (n=3).

Figure 4. TGFβ1 drives ubiquitin-independent degradation of CDCP1 by the proteasome. PhLFs were treated for 48 h with 1 ng/ml TGFβ1 together with different doses of (A) Bafilomycin and (B) Bortezomib (Bz), and the expression of CDCP1, αSMA, phospho anti-Smad3 (S423+S425), and anti-Smad3 from the whole protein lysates analyzed via immunoblot. (A) LC3B was used as a marker for autophagy. Shown is one representative blot from three independent experiments (n=3). (B) Detection of K48 polyubiquitynated (UbiK48) proteins was used as readout for proteasomal inhibition. Shown is one representative blot from six independent biological experiments (n=6). (C) Densitometric quantification of CDCP1/β-actin and αSMA/β-actin ratio from (B) presented as ± SEM. PhLFs were treated with 1ng/ml TGFβ1 and 10 nM of Bz in parallel for 48 h and subsequently analyzed for (D) ubiquitination and (E) expression of CDCP1. (D) Direct interaction of CDCP1 with UbiK48 was analyzed via pulldown of CDCP1 from whole cell lysates followed by immunoblotting for K48. Shown is one representative blot from three independent biological experiments (n=3). (E) Quantitative RT-

PCR analysis of CDCP1 and αSMA transcript levels. Data shown as ± SEM from three different fibroblast cell lines (n=3). Statistical analysis: One-way ANOVA with Bonferroni's Multiple Comparison Test. ***p<0.001, **p<0.01, *p<0.05. wo = non-treated cells, Bz = Bortezomib.

Figure 5. CDCP1 silencing affects its surface and total protein expression levels. (A) FACS analysis of reversely transfected phLFs with control or CDCP1-specific siRNAs for 48 h was used to determine the percentage of surface positive CDCP1 cells after the knockdown. Cells were labeled with APC-conjugated CDCP1 antibody and its corresponding isotype control. (B) Percentage of CDCP1 positive cells (left graph) and MFI values (right graph) after siRNA knockdown (siCDCP1) in comparison to scrambled siRNA controls (siScr). Both graphs exhibit a significant reduction of CDCP1 after siRNA silencing. The data represents the mean of eight independent experiments (n=8) with ± SEM. Statistical analysis: Paired two-tailed *t-test.* ***p<0.001, *p<0.05. (C) Immunoblotting analysis of CDCP1 and αSMA of whole cell lysates treated with various siRNA concentrations (scrambled siRNA control (scr), 2 nM, and 10 nM) for 24, 48, and 72 h. One representative blot from three independent experiments is shown (n=3).

Figure 6. Knockdown of CDCP1 increases the phosphorylation of Smad3 in the presence of TGFβ1. Cells were reversely transfected with scrambled or CDCP1-specific siRNA, and treated with or without TGFβ1 for (A) 1 h, (B) 26 h, and (C) 48 h (with a restimulation after 24 h in case of 26 and 48 h total stimulation time). Whole cell lysates were probed for CDCP1, phospho anti-Smad3 (S423+S425), anti-Smad3, and αSMA antibodies. One representative blot from six independent experiments (n=6) is shown. (D) Densitometric quantification of pSmad3/Smad3 ratios from immunoblots shown in (A), (B), and (C). Data are shown as ± SEM. Statistical analysis: One sample *t-test.* *p<0.05. (E) A luciferase reporter assay was used to investigate whether CDCP1 modulates TGFβ1 signaling in phLFs. Cells were reversely transfected with CDCP1-specific siRNA and 24h after transfection, a SMAD signaling luciferase

reporter and control construct were introduced to cells followed by TGFβ1 stimulation (1 ng/ml) for 26 h or 48 h. Shown is a summary of three independent biological experiments (n=3), measurements were performed in quadruplicates. Statistical analysis: Paired two-tailed *t-test.* *p<0.05.

Figure 7. CDCP1 inhibits TGFβ1-mediated cell adhesion of lung fibroblasts. (A) Primary human lung fibroblasts were transfected with control (siScr) or CDCP1-specific siRNA (siCDCP1), serum-starved, and stimulated with 1 ng/ml TGFβ1 every 24 h for a total of 48 h. Cells were transferred into a 48-well plate and allowed to attach for 10 min. Attached cells were immediately fixed, stained with DAPI (green) and Phalloidin (red), and each well was scanned with a confocal LSM microscope (8x8 tiles scanning area covering almost the whole well). Representative images from five independent experiments are shown. (B) Quantification and statistical evaluation of the adhesion capacity of phLFs by analyses of the images shown in (A) (n=5). The knockdown of CDCP1 significantly increases the adhesion of phLFs to the surface of the cell culture dish only in the presence of TGFβ1. Data are represented as ± SEM. Statistical analysis: One-way ANOVA with Bonferroni's Multiple Comparison Test. **p<0.01. *Scale bar*: 10 µm.

Figure 8. CDCP1 silencing increases protein expression of αSMA, collagen V, and fibronectin. PhLFs were reversely transfected with scrambled (-) and CDCP1-specific siRNA (+) followed by stimulation with 1 ng/ml TGFβ1 for 48 h. Afterwards, the expression of CDCP1, αSMA, fibronectin, and collagens in whole cell lysates was analyzed by immunoblot (A). Shown is one representative blot out of five to ten independent experiments (n=5-10). For quantification CDCP1, αSMA, and collagens' expression was normalized to β-actin (B) and data are given as ± SEM. Statistical analysis: Paired two-tailed *t-test* for a comparison of single columns. ***p<0.001, **p<0.01, *p<0.05. (C) Representative immunostainings of αSMA (green) in phLFs

763 treated with scrambled or CDCP1-specific siRNA in the presence/absence of TGFβ1 for 48 h.
764 Images were acquired by confocal microscopy scanning each well (8x8 tiles scanning area).
765 Nuclei were visualized with DAPI (white). Each image shown is representative for three
766 independent experiments (n=3). *Scale bar*: 1000 µm. (D) Representative immunofluorescent
767 costainings of CDCP1 (red) and αSMA (green) in healthy and IPF paraffin tissue sections.
768 Nuclei were counterstained with DAPI (blue). Each shown section is a representative image from
769 four different donors (n=4) and four different IPF patients (n=4). *Scale bar:* 50 µm. EF = elastic
770 fibres, MyF = myofibroblasts.

Figure 1

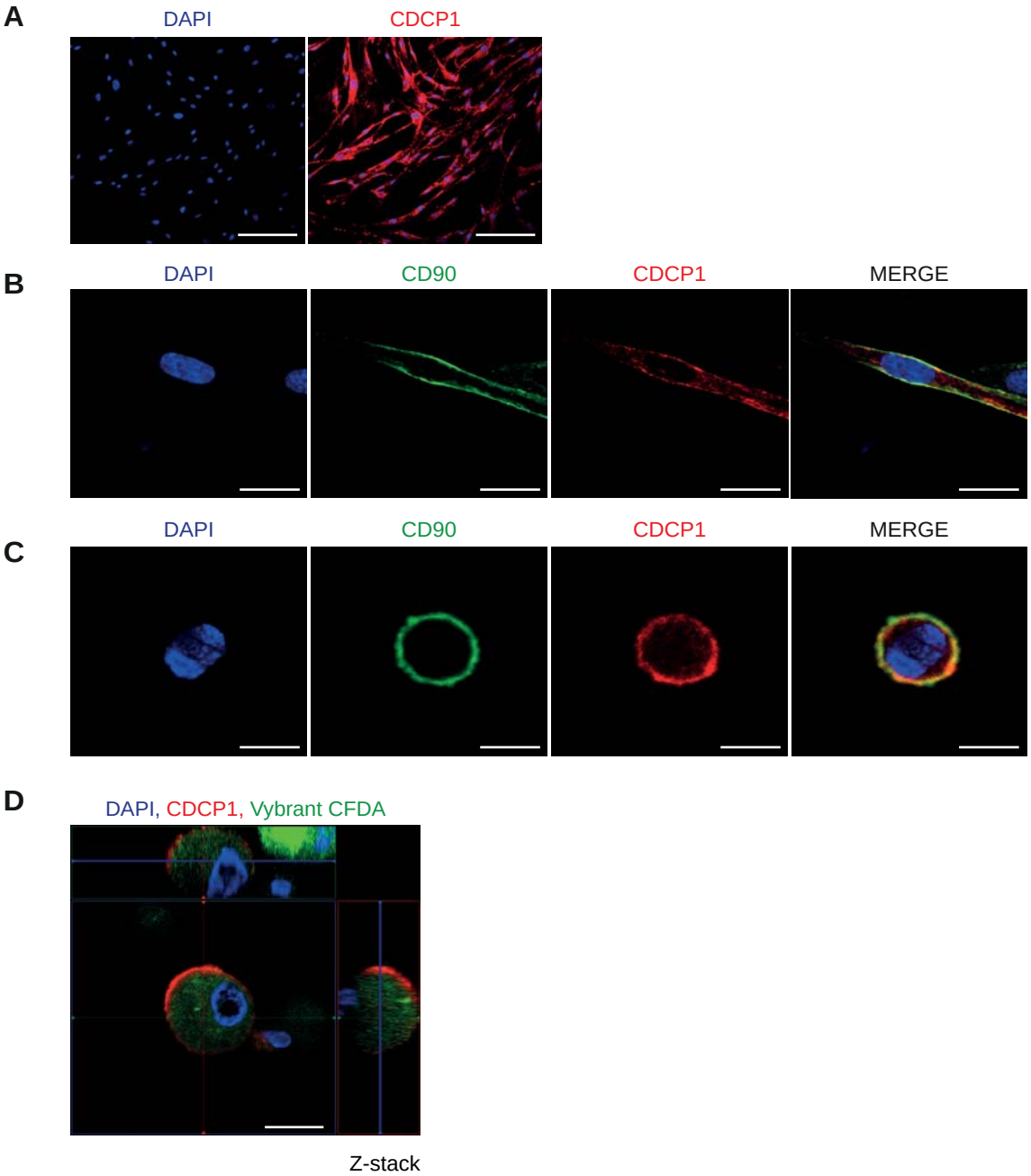

Figure 2

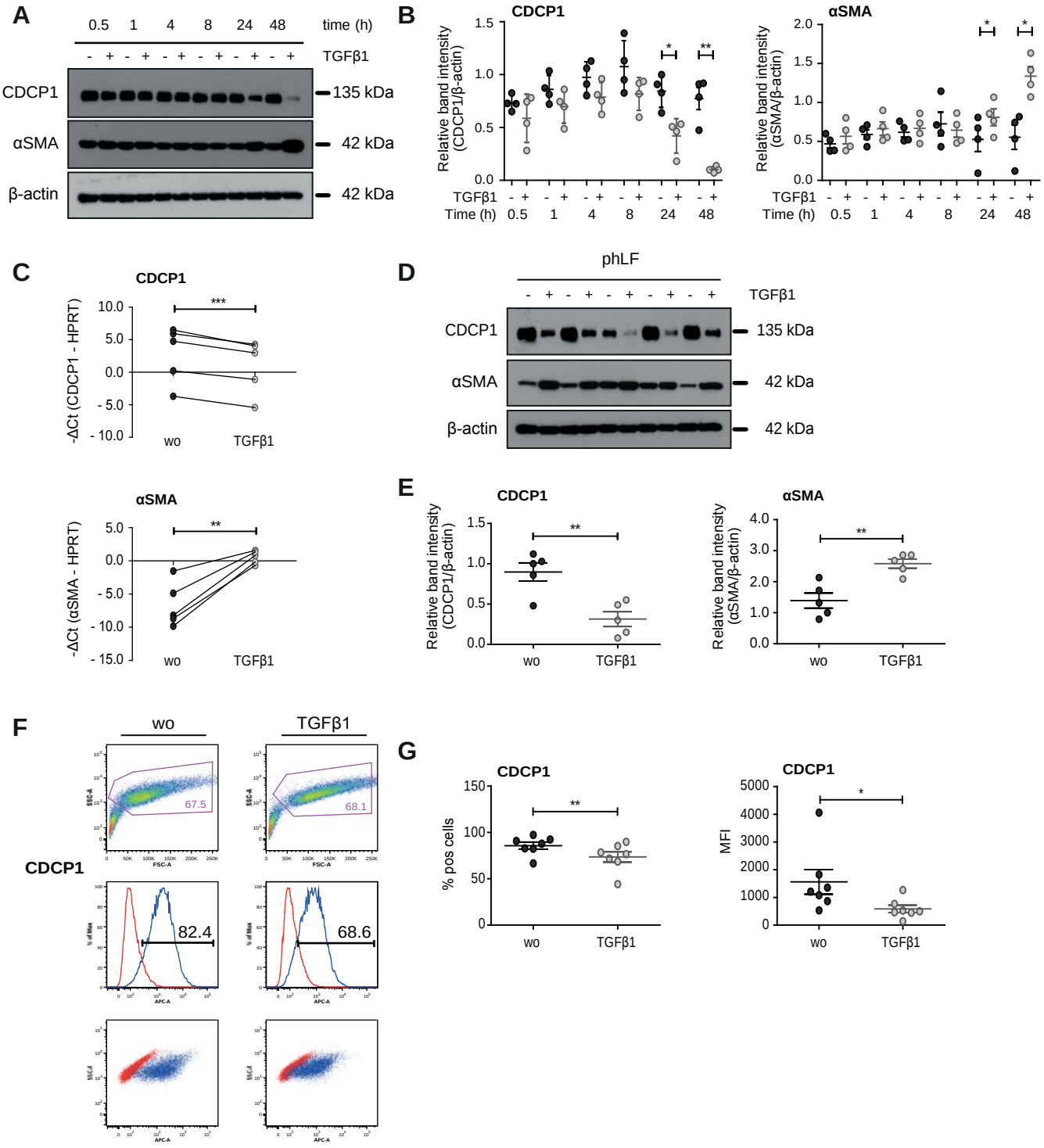

Figure 3

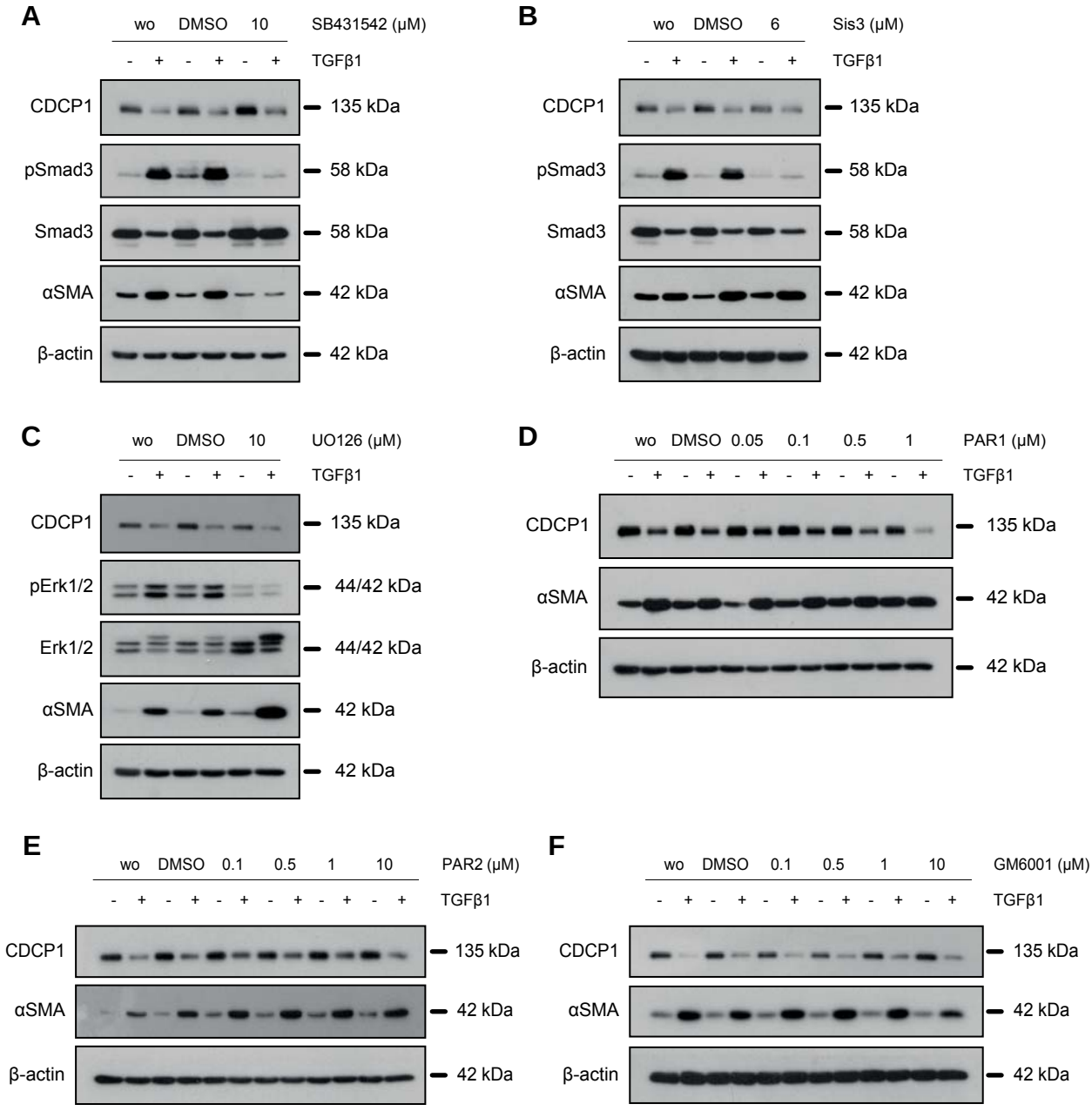

Figure 4

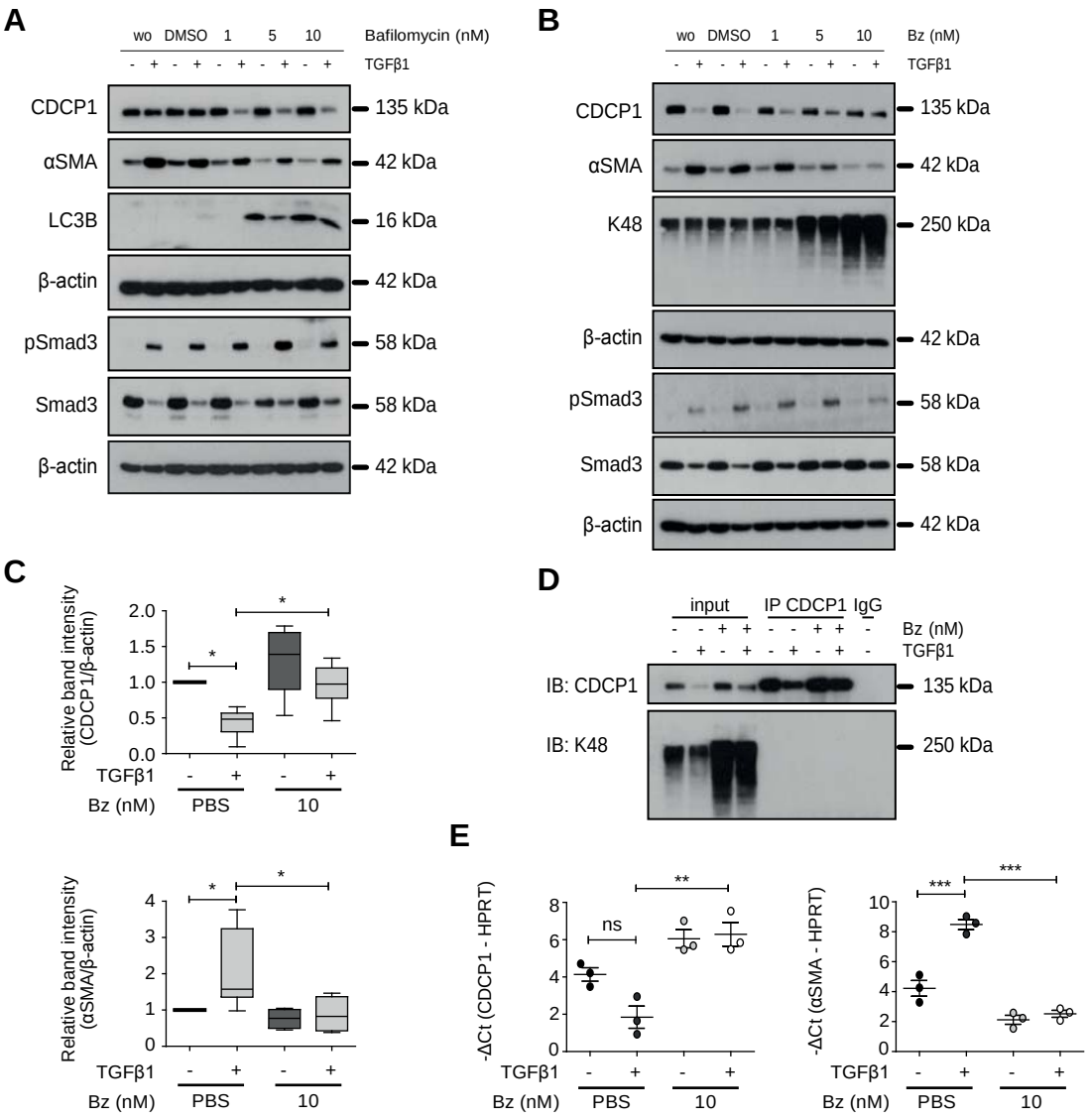

Figure 5

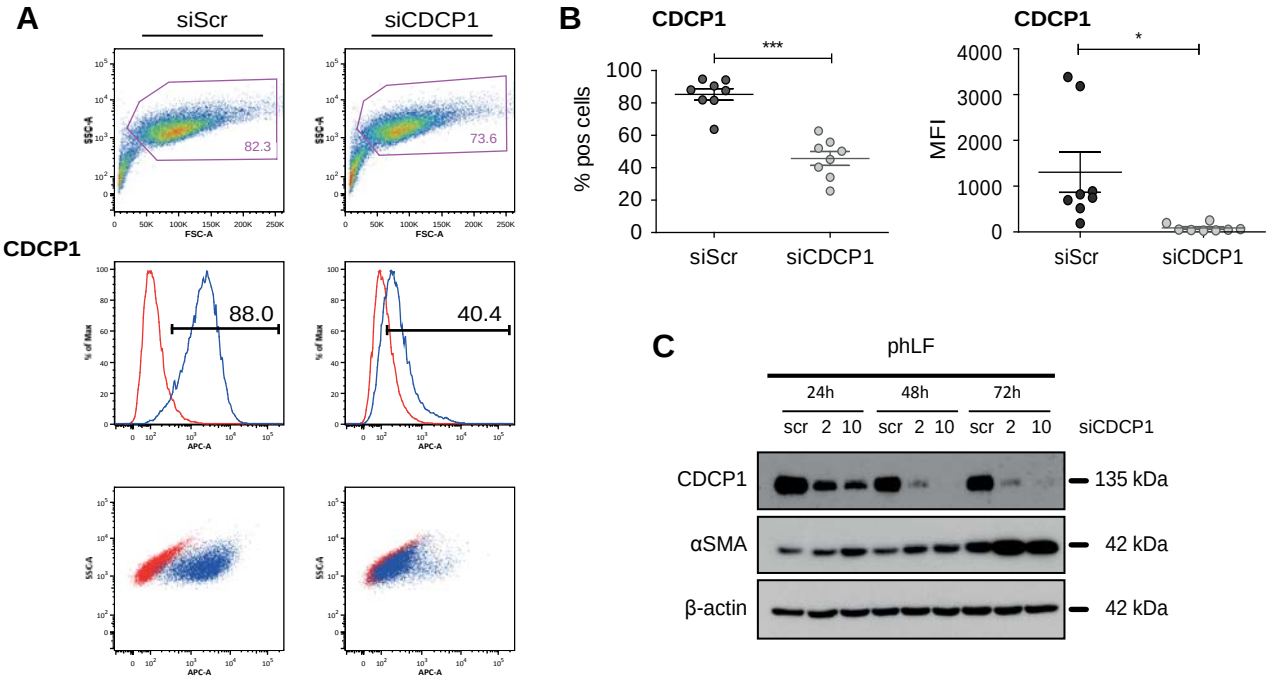

Figure 6

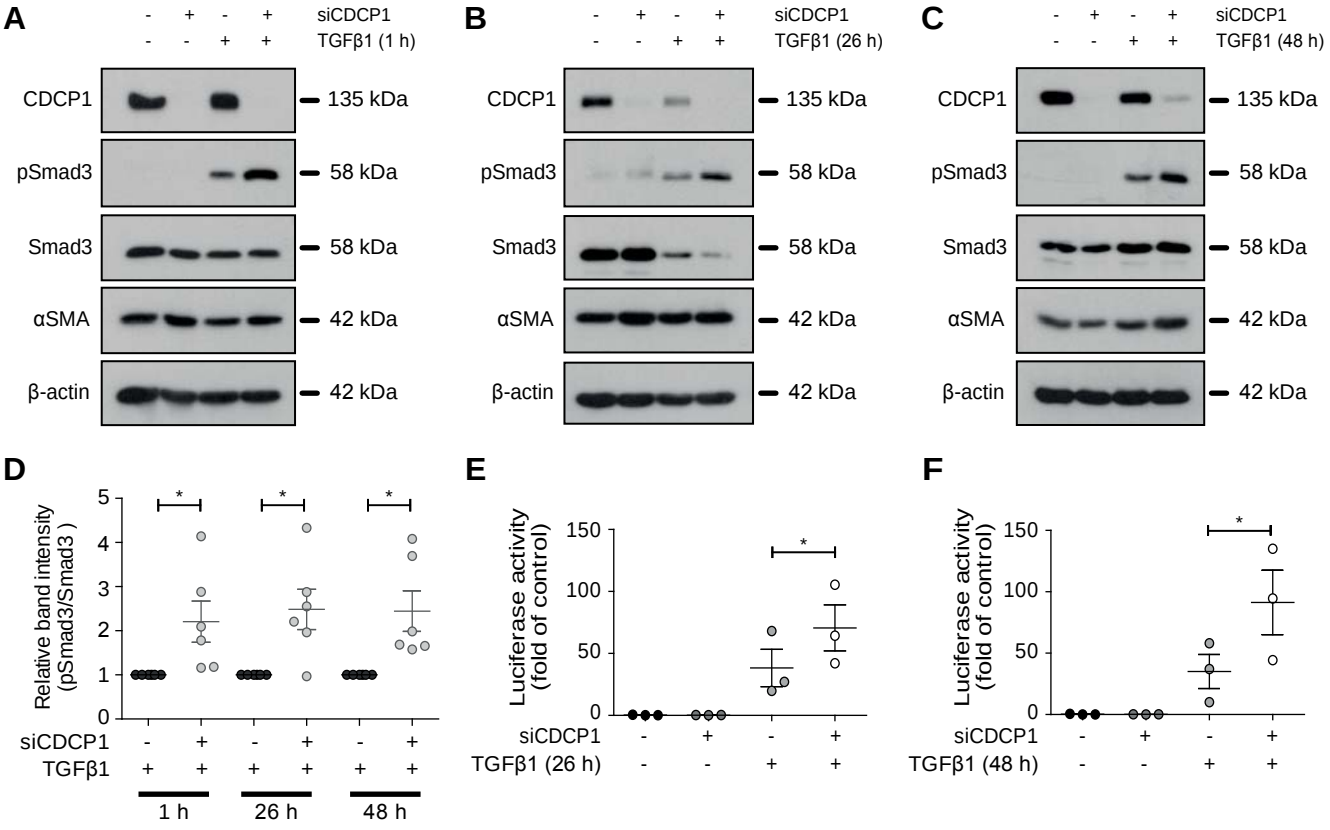

Figure 7

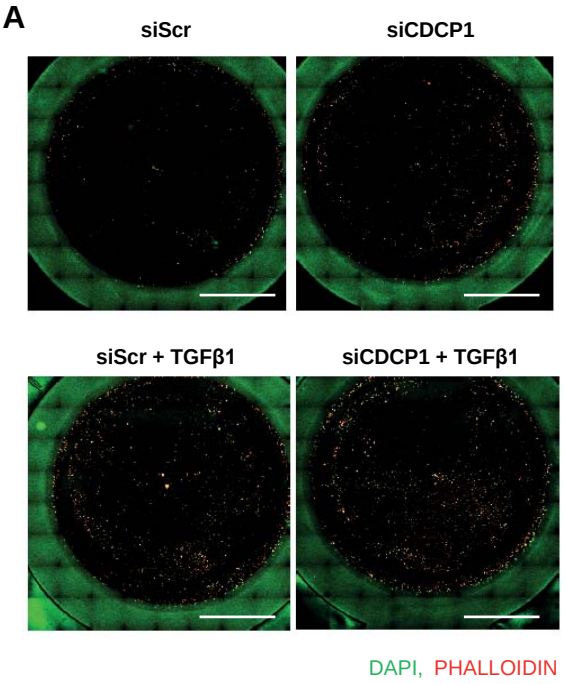

Figure 8